



Chinese Society of Aeronautics and Astronautics
& Beihang University
Chinese Journal of Aeronautics

cja@buaa.edu.cn
www.sciencedirect.com



CFD predictions of LBO limits for aero-engine combustors using fuel iterative approximation

Hu Bin ^a, Huang Yong ^b, Wang Fang ^{b,*}, Xie Fa ^b

^a Key Laboratory of Light-duty Gas-turbine, Institute of Engineering Thermophysics, Chinese Academy of Sciences, Beijing 100190, China

^b AEL Key Laboratory of Science and Technology for National Defence, School of Energy and Power Engineering, Beihang University, Beijing 100191, China

Received 9 October 2011; revised 23 April 2012; accepted 18 June 2012

Available online 16 January 2013

KEYWORDS

Aero-engine combustor;
Computational fluid dynamics;
Fuel iterative approximation;
LBO limits prediction;
Perfect stirred reactor

Abstract Lean blow-out (LBO) is critical to operational performance of combustion systems in propulsion and power generation. Current predictive tools for LBO limits are based on decades-old empirical correlations that have limited applicability for modern combustor designs. According to the Lefebvre's model for LBO and classical perfect stirred reactor (PSR) concept, a load parameter (LP) is proposed for LBO analysis of aero-engine combustors in this paper. The parameters contained in load parameter are all estimated from the non-reacting flow field of a combustor that is obtained by numerical simulation. Additionally, based on the load parameter, a method of fuel iterative approximation (FIA) is proposed to predict the LBO limit of the combustor. Compared with experimental data for 19 combustors, it is found that load parameter can represent the actual combustion load of the combustor near LBO and have good relativity with LBO fuel/air ratio (FAR). The LBO FAR obtained by FIA shows good agreement with experimental data, the maximum prediction uncertainty of FIA is about $\pm 17.5\%$. Because only the non-reacting flow is simulated, the time cost of the LBO limit prediction using FIA is relatively low (about 6 h for one combustor with computer equipment of CPU 2.66 GHz \times 4 and 4 GB memory), showing that FIA is reliable and efficient to be used for practical applications.

© 2013 CSAA & BUAA. Production and hosting by Elsevier Ltd.
Open access under [CC BY-NC-ND license](http://creativecommons.org/licenses/by-nc-nd/3.0/).

1. Introduction

In aero-engine applications, lean blow-out (LBO) plays a critical role in the operational envelope of engines. Aero-engine combustors sometimes operate at very low inlet pressure and fuel/air ratios (FARs) that lie outside the normal flammable limits of hydrocarbon-air mixtures.¹ Generally, a LBO FAR of 0.005 for combustors is needed to avoid blow-out during rapid engine deceleration at altitude, as well as to maintain combustion during high altitude relight. LBO prediction tools available in the industry today are based on components testing along with generic and simplified correlations, which need

* Corresponding author. Tel.: +86 10 82339356.

E-mail addresses: iamhubin@yahoo.com.cn (B. Hu), fwang@buaa.edu.cn (F. Wang).

Peer review under responsibility of Editorial Committee of CJA.



Production and hosting by Elsevier

high costs and understandably have limited applicability for modern combustor designs, especially for the state-of-the-art systems that push the performance envelope. With rapid development of numerical simulations in recent years, computational fluid dynamics (CFD) has provided new insight into the fundamental processes that occur in these flows. Recent data have even allowed flame dynamics near LBO to be directly observed with high spatial and temporal resolutions. How to predict the LBO limit of a combustor efficiently and accurately based on numerical simulations has become a research focus in the application of combustion engineering.

At present, there are lots of theoretical models for LBO. Most of them can be classified into two categories: perfect stirred reactor (PSR)^{2,3} models and characteristic time (CT) models.⁴ Both of them originated from early studies of stabilization of bluff-body flames. Afterwards, PSR and CT models were improved by Refs.⁵⁻¹¹ so that they could be used in LBO predictions of aero-engine combustors. The difference between PSR and CT models is that PSR models are established based on energy balance and CT models on time balance.

Rizk and Mongia¹² combined the Lefebvre's model for LBO with 3D computer codes. The 3D computations were applied to a combustor domain which was divided into a large number of finite difference nodes along axial, radial, and circumferential directions. It was needed to run at two power conditions (47% and full power) to determine the empirical constants, and then the codes could be used in LBO predictions at other power levels. Because the partial actual LBO data must be obtained in advance, these "predictions" are really correlations.

Another hybrid modeling approach for LBO predictions was presented by Refs.¹³⁻¹⁵. The procedure began with a CFD calculation at representative operating conditions of interest. The field solutions resulting from the CFD calculation were post-processed using a dissipation gradient analysis and topological methods to represent the fluid dynamics by means of a connected network of fuel/air mixers, PSRs, and plug-flow reactors. Detailed chemistry was solved on the network over the required range of operating conditions near LBO to yield the desired solutions.

Black and Smith¹⁶ studied the transient LBO of a low emission injector using unsteady Reynolds averaged Navier–Stokes (URANS) and large eddy simulation (LES). It was shown that URANS could embody the basic characteristics of transient LBO, but the predictions obtained by URANS could not match the experimental data for any configurations. The LES simulations demonstrated that the accurate representation of the fuel distribution in the injector would be critical. However, capturing these effects would require appropriate atomization and dispersion models working in conjunction with combustion LES. Hence, along with additional model development, validation simulations of different configurations would be required to demonstrate the accuracy and effectiveness of using numerical methods for LBO predictions.

Menon and his group^{17,18} considered that local extinction played an important role in the process of LBO and used a combined model LES + LEM (Linear Eddy Mixing) to study the effects of different vortexes scales on local extinction. The results showed that not all the vortexes but only vortexes in a specific scale affected the local extinction. Although numerical simulations could capture the flame distortion and variation of flame spread velocity, they were unable to capture the vortexes which

had great effects on local extinction. So the relevant numerical simulation methods still need to be improved.

Kim et al.¹⁹ studied the turbulent reacting flows behind a bluff-body flame holder using LES and a simple combustion model of eddy break-up model (EBU). It showed an encouraging result that the LBO FAR obtained by this model could match the experiment data. However, the result was only confined in one combustor configuration, which could be problematic when applying this model for other configurations and conditions. Additionally, for a simple combustor with no liner, a typical LES calculation requires 20 d using 16900 MHz PCs, and the time would be dramatically increased when LES is used for aero-engine combustors. It is absolutely not acceptable, especially in the design stage of combustors.

A series of studies on V-gutter flame stabilization were also operated by Kanus,^{20,21} Smith,²² Wang²³ and Roach et al.²⁴ using local Damköhler number (Da). This approach would raise many questions on how this methodology should be implemented. For example, what are the critical locations in an afterburner that determine stability? What temperature should be used when making ignition delay calculations? When can the perfect mixing assumption be applied, and when should a PSR reactor be used? Shanbhogue et al.²⁵ also considered that the Da model could properly demonstrate the local extinction in the process of LBO, but it was not proper for the entire extinction.

From the discussion above, it is known that a single numerical simulation with high spatial and temporal resolutions cannot be used efficiently in LBO predictions due to computational costs and complexity. Additionally, the combustion numerical simulation is usually competent for the solution of combustion in stable conditions but not able to accurately calculate the transient conditions yet because of its own limitations such as multi-step reaction, applicability of Arrhenius law and pseudo diffusion, etc.²⁶ Currently, relevant computational models still need to be improved to quantitatively predict LBO limits of combustors.

2. Motivation

The objective of this research is to develop a new methodology for LBO limit predictions based on PSR concept and numerical simulations, so that it allows researchers quickly and accurately evaluate the LBO limit only from the cold flow field of a combustor.

The research idea is originated from the analysis of the Lefebvre's model for LBO. For heterogeneous mixtures (liquid fuel), the overall FAR at LBO is expressed as:⁷

$$q_{\text{LBO}} = \left(\frac{A' f_{\text{PZ}}}{V_c} \right) \left(\frac{m_a}{p_3^{1.3} \exp(T_3/300)} \right) \left(\frac{D_r^2}{\lambda_r H_r} \right) \left(\frac{D_{0,T_f}}{D_{0,277.5\text{K}}} \right) \quad (1)$$

where f_{PZ} represents the fraction of the evaporated fuel in primary zone, V_c the combustor volume ahead of dilution holes, A' the combustor configuration parameter, m_a total mass flow rate of combustor inlet, p_3 inlet pressure, D_r the initial diameter of droplet; λ_r and H_r represent effective evaporation constant and lower calorific value, D_{0,T_f} and $D_{0,277.5\text{K}}$ account for the variations in drop sizes from the baseline fuel temperature of 277.5 K.

By the experimental validation of eight kinds of aero-engine combustors, Lefebvre considered Eq. (1) to be universal

because the value of A/f_{PZ} kept nearly constant at 29 for these combustors. The prediction uncertainty of Eq. (1) was claimed to be $\pm 30\%$.

It is not difficult to find that V_c (combustor volume ahead of dilution holes) is the only combustor configuration parameter contained in Eq. (1). It is questionable that the LBO FAR of different combustors would be equivalent if they have the same V_c . In author's previous combustion visual experiment,²⁷ it was found that the actual combustion zone near LBO was changing in different combustors and not consist with V_c defined in the Lefebvre's model. Meanwhile, the change of combustion volume would correspondingly cause the variation of the flow rate of combustion air. For these reasons, the global inputs of V_c and m_a included in the Lefebvre's model may be problematic when Eq. (1) is used in other kinds of combustors.

On the other hand, it is understandable that once the inlet condition, combustor structure, and properties of fuel are fixed, q_{LBO} should be determined and independent of whether the incoming flow is ignited, that is, the LBO performance (q_{LBO}) and cold flow field of the combustor should be related. Therefore, it is greatly possible to evaluate the LBO performance only from the cold flow field of the combustor. Because of this, only numerical simulations of cold flows (velocity field and concentration field) in the combustor are operated in this study.

According to the above two points and classical PSR concept, a load parameter of $V_f \cdot m_f$ is proposed for LBO analysis in the present study. V_f and m_f are all estimated from the cold flow field of the combustor. V_f represents the flammable (or combustion) volume and is defined by flammable limit. The mass flow rate of back-flow air which enters the flammable zone (m_r) is used to account for the combustion air. However, the load parameter of $V_f \cdot m_r$ cannot be directly used in LBO predictions due to V_f is strongly affected by mass flow rate of fuel m_f . For this reason, a new method of fuel iterative approximation (FIA) is established. The iterative value $q_{LBO,n}$ will approximate to q_{LBO} infinitely when $n \rightarrow +\infty$ that will be discussed in detail in Section 6.

3. Experiment setup

The LBO experiments are operated on a single dome (1/18 of the annular combustor) rectangular model combustor with dual-radial/axial-radial/dual-axial swirl cup in the Fundamental Combustion Laboratory (FCL) of Beihang University (BUAA) (see Fig. 1).

19 model combustors with different combinations of components are covered in this study. The model combustor contains four components and each component has alternative designs: swirl-cups assembly (dual-axial/axial-radial/dual-radial), venturi (different throat curvatures), flare (different outlet angles), and primary holes (different hole arrangements under the same intake area). The general configuration and main parameters of each combustor are shown in Table 1. In Table 1, A_{pri} and A_{sec} are the effective area of primary swirler and secondary swirler, r_1 and r_2 are the curvature radius upstream and downstream from the venturi throat, d is the diameter of venturi throat, δ is the outlet angle of flare.

The LBO FAR is obtained as follows: stable combustion is established at a fixed air mass flow rate, and then the fuel flow is reduced slowly until extinction occurs. Once extinction is achieved, the final fuel flow rate is recorded. The fuel employed in experiment is Chinese RP-3 kerosene (similar to JP-8).



Fig. 1 LBO test rig and dual-axial/axial-radial/dual-radial swirl-cup assemblies.

The experimental uncertainties mainly come from the following aspects: (1) instruments; (2) manual adjustment; (3) signal acquisition; (4) calibration, and so on.

Since LBO limit is defined as the ratio of the fuel flow and the air flow at LBO, the relative uncertainty of the LBO limit is comprised of the relative uncertainty of the fuel flow and the relative uncertainty of the air flow. The air flow's uncertainty consists of the calibrated uncertainty of the air flow meter, instruments' uncertainty, and manual adjustment uncertainty. The fuel flow's uncertainty consists of the calibrated uncertainty of the fuel injector, instruments' uncertainty, and manual adjustment uncertainty, and so on. Therefore, the relative uncertainty of the LBO limits is obtained by the sum of the above relative uncertainties. The results show that the measurement uncertainty of the LBO limits is within 4%.

4. Computation

4.1. Turbulent model

RANS is used in the present study because the average flow is the main concern instead of the instantaneous flow in the combustor.

Turbulent model of realizable $k-\epsilon$ is used. The realizable $k-\epsilon$ model has been developed recently to be used extensively in the solution of swirling flows. A remarkable advantage of the realizable $k-\epsilon$ model is to accurately predict the flows involving rotation, boundary layers under strong adverse pressure gradients, separation, and recirculation. The relevant parameters contained in the realizable $k-\epsilon$ model are listed in Table 2. The specific meanings of these parameters are given in Ref. 28.

4.2. Computational domain and boundary conditions

Fig. 2 shows the computational domain and numerical boundary conditions.

At the air inlet, the mass flow is 0.589 kg/s. The air temperature and gauge pressure in the air inlet are 300 K and 230 kPa, respectively. The method of inlet turbulent specification is turbulent intensity (10%) and length scale. In Fluent, turbulent length scale is characterized by the inlet hydraulic diameter (36.34 mm) defined as $D_H = 4A_c/C_w$ (where A_c is the cross sectional area, C_w wetted perimeter of cross-section, D_H hydraulic diameter). Pressure outlet boundary condition (220 kPa) is used for the outlet. The back-flow turbulent intensity and hydraulic diameter at the outlet are 10% and 65.62 mm, respectively. Standard wall function is used for near-wall treatment. The mass flow rate of fuel m_f (kerosene vapor) is obtained from LBO experiment. Second order upwind scheme is used in all cases.

Table 1 Combustor configurations and parameters.

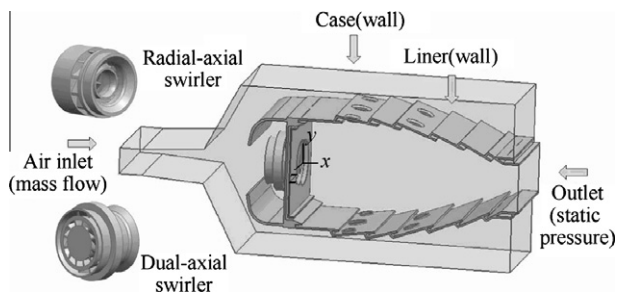
Combustor labels	Swirl-cups		Venturi			Flare	Primary hole arrangements
	Type	A_{pr}/mm^2	A_{sec}/mm^2	r_1/mm	r_2/mm	d/mm	
1		147.5	186.6				
2		111.4	186.6				45
3		147.5	223.0				
4		147.5	186.6	6.3	6.3		35
5	Dual-axial	147.5	186.6			18.5	
6		178.8	186.6				
7		147.5	150.4				
8		147.5	186.6				
9		147.5	186.6	14	4		
10		113.3	190.7	6.3	6.3		
11	Axial-radial	144.6	190.7	14	4		
12		144.6	190.7				45
13		146.7	190.7				
14		73.35	190.7				
15		73.35	95.35	6.3	6.3		13
16	Dual-radial	146.7	190.7				
17		73.35	190.7				
18		146.7	95.35				
19		73.35	95.35				

Table 2 Model parameters contained in realizable $k-\varepsilon$ model.

C2-epsilon	Turbulent kinetic energy Prandtl number	Turbulent eddy dissipation Prandtl number	Energy Prandtl number	Wall Prandtl number
1.9	1	1.2	0.85	0.85

4.3. Grid generation

The grids are generated by commercial software Gambit. Due to the complicated configuration of a combustor, the computa-

**Fig. 2** Computational domain and numerical boundary conditions.

tional domain is divided into lots of small parts. Tetrahedral grids are generated in/around the dome and the liner. The others are generated in hexahedral grids. The grids scale is about 1 mm, and the sum of the grids is about 3.5 million. The computational grids are shown in Fig. 3.

4.4. Validation

A validation computation of the numerical simulation methods used in the present study is operated on a model combustor assembled with an axial swirl-cup. The computational domain is shown in Fig. 4. The flow field in the model combustor is non-reacting and measured by Davoudzadeh et al.²⁹ using laser Doppler velocimetry (LDV). Meanwhile, a corresponding computational study is also conducted by Davoudzadeh et al.²⁹ as a comparison with the experimental data.

The boundary conditions set in the numerical simulation are consistent to the LBO experiment. Incoming velocity is

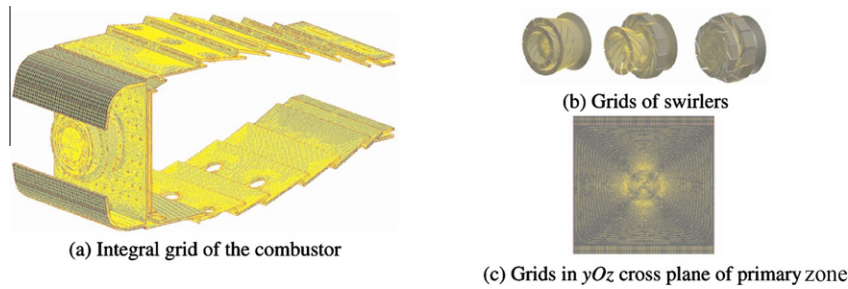


Fig. 3 Various views of computational grids.

20.14 m/s, and the gauge pressure and static temperature of the incoming air are 1 MPa and 300 K, respectively.

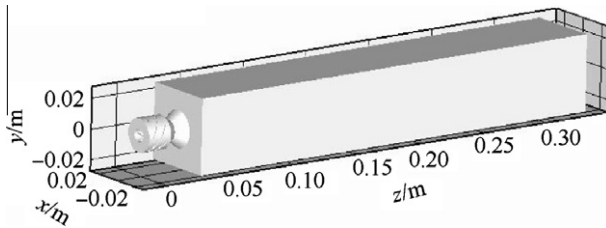


Fig. 4 Computational domain of the model combustor for validation.

Fig. 5 is the comparison of the computational results obtained in the present study with the experimental and computational results obtained by Davoudzadeh et al.²⁹ Fig. 5(a) is the distribution of the axial velocity along the centerline in the combustor; Fig. 5(b–h) are the profiles of the axial velocity in different locations ($\Delta z = 3, 6, 9, 12, 24, 36$ and 48 mm) downstream from the swirler.

Fig. 5 reveals that the computational results operated in the present study fit satisfactorily with experiment data ($r > 0.88$) and are better than those operated by Davoudzadeh et al.²⁹ It is shown that the numerical simulation method used in this paper is reliable and applicable for the solution of flows in combustors.

5. Load parameter for LBO analysis

In view of the load parameters for LBO predictions, two commonly used empirical parameters are $\frac{U}{p^{0.95}D^{0.85}}$ and $p^{0.324}T^{1.07}(750 - U)^{0.252}$ that are derived by Dezubay³⁰ and King,³¹ respectively. They are all derived from the analysis of bluff-body stabilized flames. Similarly, if some proper parameters or combined parameters could be estimated from the flow field of aero-engine combustors and have good corresponding relation to the LBO performance (q_{LBO}), it is greatly possible to develop a simple and accurate LBO predicting method that allows engineers evaluate the LBO performance of combustors in short time, especially in the designing stage of combustors.

5.1. PSR concept in combustors

It is well known that combustion air and combustion volume are two important parameters related to combustion performance in classical PSR theory. Previous combustion visual

experiment²⁷ shows that the LBO limit is deteriorated as the increase of flame volume near LBO (see Fig. 6). It is contrary to the Lefebvre's model in which the combustion volume is in inverse proportion to LBO FARs.

A smaller flame volume represents worse fuel/air mixing within the whole combustor. That is good for flame stabilization because the local rich zone will ignite the adjacent region where the FAR is lower than flammable limit, and then it will not cause entire extinction in the combustor. For this reason, the combustion volume seems to be proportional to q_{LBO} .

Since flame can only propagate within a certain range, the flame volume is defined by the lean flammable limit of the fuel based on the numerical simulation results of the non-reacting flow in the combustor in this paper. That is so long as the region where the fuel mass fraction is higher than lean flammable limit is considered to be the flame (or combustion) volume. This combustion volume is named flammable volume (V_f) here.

Theoretically, the combustion air (m_c) should be the air enters the combustion zone (V_f), which contains part of the air from primary swirler, secondary swirler, primary holes, and cooling holes in the dome. However, in the flow field without combustion, it is difficult to calculate m_c . Some of the air that enters the V_f would be computed repeatedly due to the back-flow. In this study, m_r is used instead of m_c which will be discussed in detail in Section 5.3.

A PSR model is established downstream the swirl cup in the primary zone as shown in Fig. 7. The combustion zone near LBO is assumed to be a PSR, and fuel and air are well stirred in the combustion zone due to the strong swirl. In accordance with the PSR model, a load parameter of $V_f \cdot m_r$ which represents the actual combustion load near LBO is also proposed. V_f and m_r are all estimated from the numerical simulation results of the cold flow field in the combustor. A bigger load parameter means a heavier combustion load which will deteriorate the LBO limit, and vice versa.

5.2. Flammable volume

It is well known that flammable limits are strongly affected by temperature. Because the temperature of incoming air in all experiments is maintained at approximately 300 K, a lean limit of kerosene of 0.03313 (at 300 K, fuel/air ratio)³² is used in V_f calculation.

Fig. 8 compares the flammable volume and flame zone obtained by numerical simulation and experiment, respectively.

The shape of the flammable zone obtained by numerical simulation looks like a horn close to the atomizer. Because

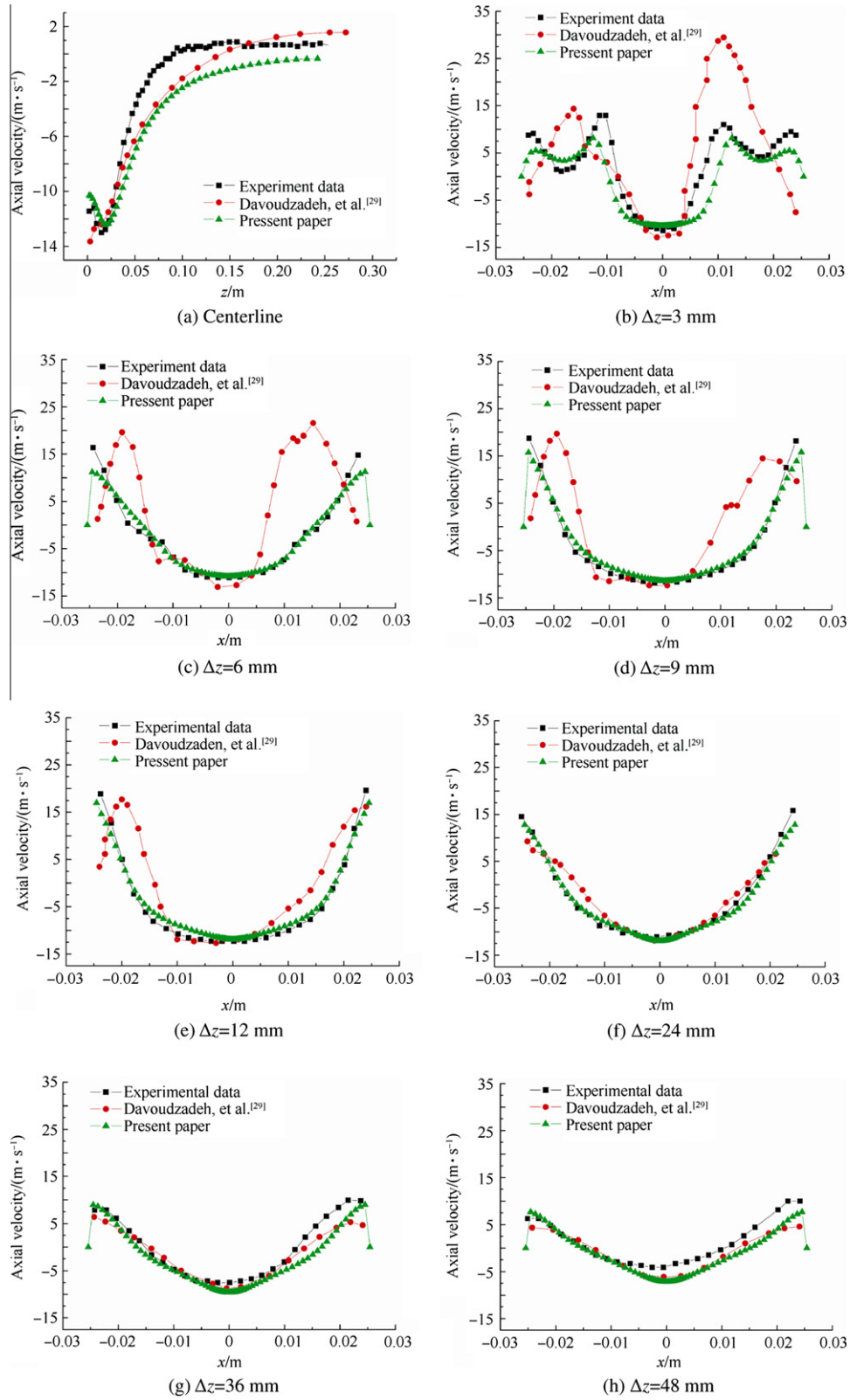


Fig. 5 Comparison of the computational results operated in the present study with experimental and computational results operated by Davoudzadeh et al.²⁹

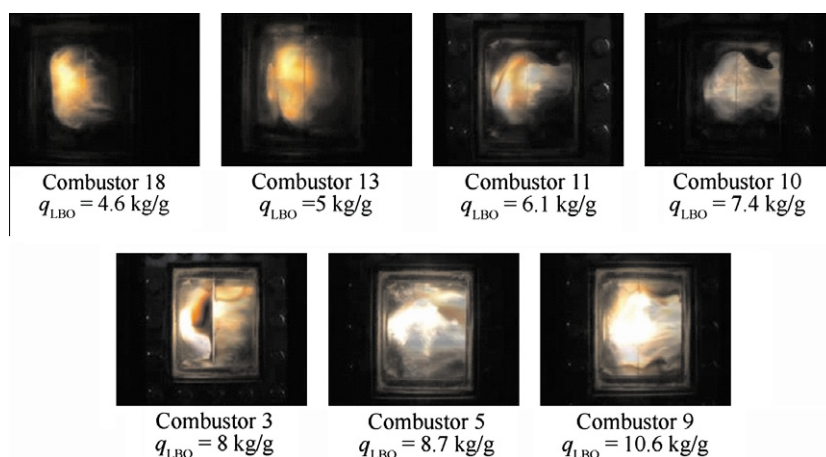


Fig. 6 Flame images of different combustors near LBO (obtained by optical camera).

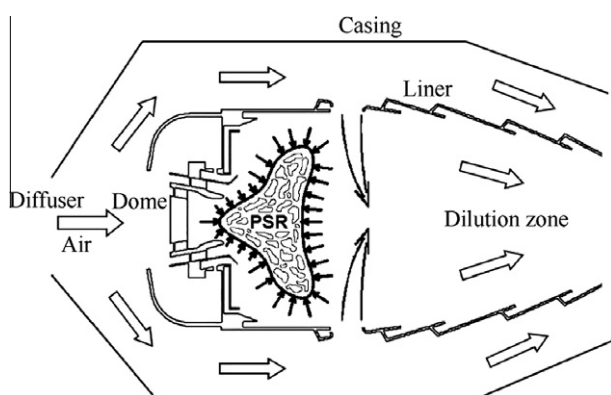


Fig. 7 Schematic of the PSR model in the combustor.

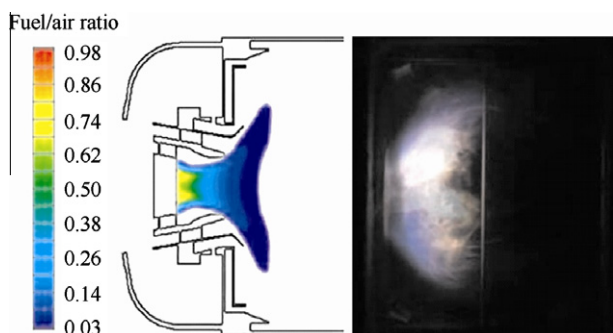


Fig. 8 Comparison between flammable volume and flame zone obtained by numerical simulation and experiment.

of the neglect of atomization and evaporation, the flammable zone (V_f) obtained by numerical simulation is relatively smaller than the flame in the experiment image.

Fig. 9 reveals that V_f increases linearly with increasing q_{LBO} . Because the m_f set in numerical simulation is obtained from the LBO experiment, the increase of q_{LBO} causes the increase of fuel flow rate, and then enlarge the V_f . In addition, another reason is that the larger flame volume represents better fuel/air mixing within the whole combustor

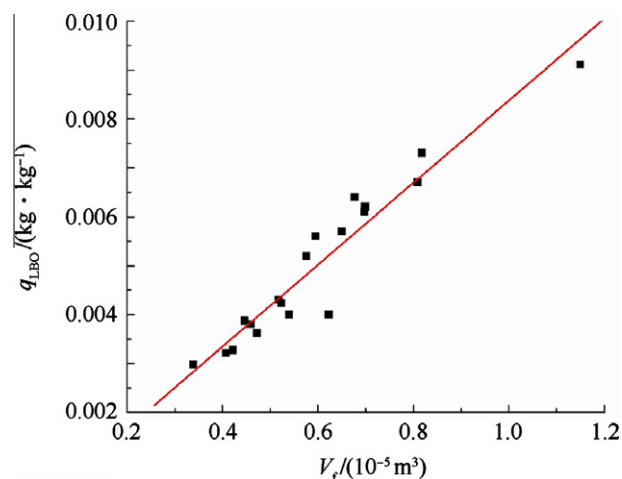


Fig. 9 Relationship between flammable volumes and LBO (FARs).

that is no good for LBO performance. Hence the LBO limits are deteriorated.

5.3. Combustion air

Fig. 10 shows the schematic of the effects of back-flow on LBO process of the combustor. Under the design point condition, the local FAR in the primary zone is close to stoichiometric. The recirculation zone contains mainly burnt gas with high temperature that supplies enough heat to ignite incoming fresh mixture. The temperature in the recirculation zone decreases with decreasing fuel mass flow rate. Simultaneously, the fraction of the fresh air in the primary zone is increased, and excess to stoichiometry. The excessive air further reduces the local FAR in the combustion zone that is not conducive to LBO performance. Therefore, the amount of back-flow gas near LBO has great effects on q_{LBO} .

It is needed to explain that the back-flow rate in either combustion flow field or cold flow field should have the same tendency of effect on q_{LBO} because it is mainly affected by the combustor configuration.

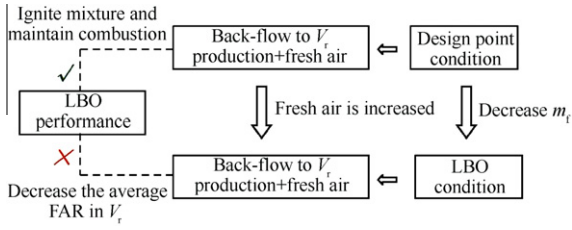


Fig. 10 Schematic of the effects of back-flow on LBO limit.

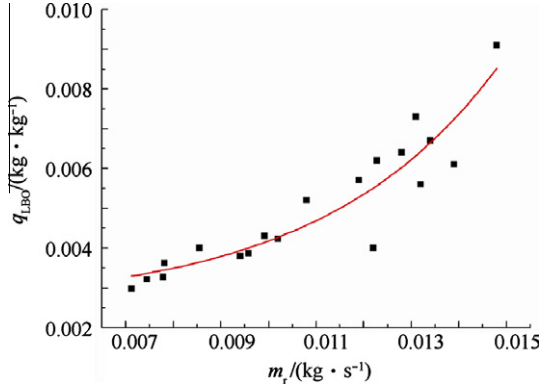


Fig. 11 Relationship between back-flow rates and LBO fuel/air ratios.

In this study, m_r is introduced into LBO analysis. Because the incoming flow is not ignited, the back-flow is only fresh air and gaseous kerosene. m_r can be obtained by computing the mass flow rate across the negative velocity face of V_f . The comparison between m_r and q_{LBO} is shown in Fig. 11. It shows an exponential relation between m_r and q_{LBO} that fully demonstrates the effects of back-flow on LBO.

5.4. Load parameter for LBO

The load parameter is obtained by the combination of V_f and m_r . The relationship of q_{LBO} and load parameter is shown in Fig. 12. It shows a good relativity between $V_f \cdot m_r$ and q_{LBO} .

The load parameter can represent the actual combustion load of the combustor near LBO. A higher load parameter means a heavier combustion load which deteriorates the LBO limit and vice versa. What is more important is that the load parameter relates the cold flow field to the LBO performance (q_{LBO}) of the combustor that is very useful to the next study of predicting the LBO limit based on the cold flow field of the combustor using FIA as discussed in Section 6.

The fitting correlation between $V_f \cdot m_r$ and q_{LBO} is expressed as follows:

$$q_{LBO} = 0.00129 + 45196.88(V_f \cdot m_r) \quad (2)$$

A relative simple correlation between q_{LBO} and $V_f \cdot m_r$ is established. The specific physical meanings of the constants contained in Eq. (2) are not clear now. Because the effects of fuel performance and atomization/evaporation are not included in the load parameter, Eq. (2) may not be universal to other fuels. To achieve this target, more experiments and computations are needed in the future.

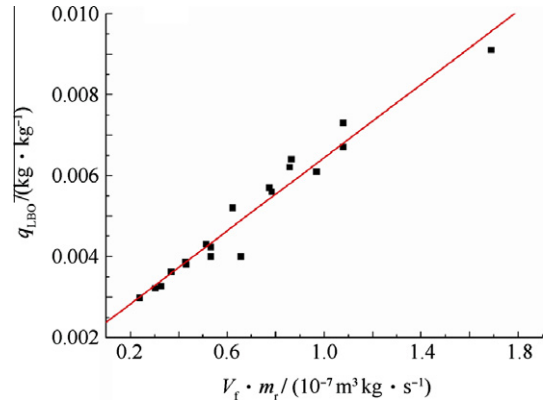


Fig. 12 Relationship between load parameters and LBO fuel/air ratios.

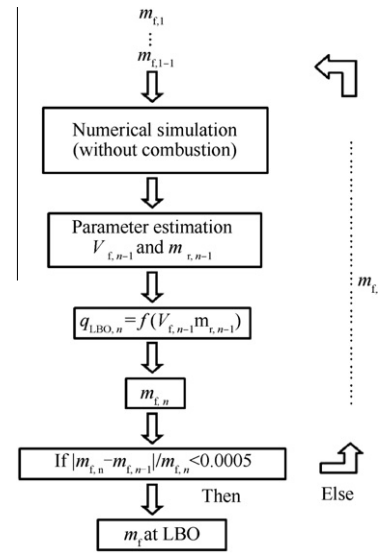


Fig. 13 Schematic of FIA for LBO prediction.

6. Load parameter for LBO prediction

6.1. LBO prediction using FIA

Eq. (2) could not be used in LBO limit predictions directly due to m_r must be obtained in advance. For this reason, a FIA method is proposed to make LBO predictions. Eq. (2) is rewritten as:

$$q_{LBO,n} = 0.00129 + 45196.88(V_{f,n-1} \cdot m_{r,n-1}) \quad (3)$$

The predicting process is demonstrated in Fig. 13.

- (1) Set the initial fuel mass flow rate $m_{f,0}$, and then solve the velocity and concentration field of the combustor without combustion.
- (2) Based on the computational results in Step (1), $V_{f,0}$ and $m_{r,0}$ can be obtained from flammable limit and mass flow integral, respectively (as discussed in Section 5).
- (3) A new fuel mass flow rate $m_{f,1}$ can be obtained based on Eq. (3). If $|m_{f,n} - m_{f,n-1}| / m_{f,n-1} < 0.0005$, $m_{f,n}$ namely is the fuel mass flow rate at LBO. Otherwise, reset the fuel mass flow rate as $m_{f,1}$ and repeat Step (2). Theoretically,

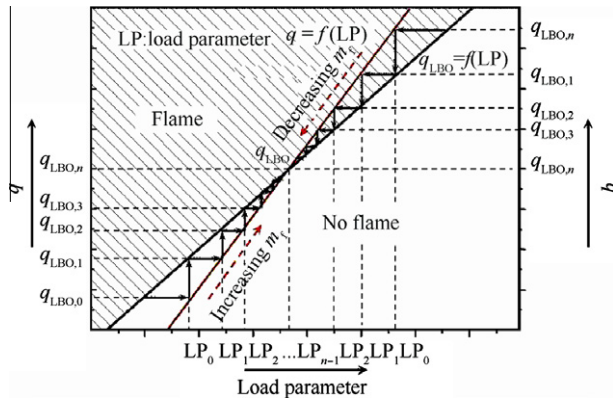


Fig. 14 Schematic of convergent mechanism of FIA.

$m_{f,0}$ can be set at random. In order to accelerate the convergent rate of $m_{f,n}$, the $m_{f,0}$ selection of equivalent ratio of 0.5 in the primary zone is recommended.

6.2. Convergent mechanism of FIA

Fig. 14 shows the schematic of the convergent mechanism of FIA. The line expressed as $q = f(LP)$ represents the correlation of q and the load parameter (LP) in a certain combustor to be predicted. For any combustors, the equation of $q = f(LP)$ can be easily obtained by data fitting through calculating the load parameter under different m_f in the numerical simulation of the non-reacting flows of the combustor. The line expressed as $q_{LBO} = f(LP)$ represents the correlation of q_{LBO} and the load parameters of 19 combustors discussed in the present study. The intersection of these two lines represents the LBO condition of the certain combustor. Fig. 14 shows the amplified relative position of two function lines near the intersection. The shadow region above $q_{LBO} = f(LP)$ represents the stable combustion zone which means that so long as the load parameter calculated

from the non-reacting flow of the combustor locates within this region, the combustion would be maintained. Otherwise, extinction would occur. The iterative process of $q_{LBO,n}$ in FIA is demonstrated by arrow lines. According to $q = f(LP)$ and $q_{LBO} = f(LP)$, LP_{n-1} and $q_{LBO,n}$ can be obtained alternately that cause $q_{LBO,n}$ eventually approach to q_{LBO} when $n \rightarrow +\infty$.

It is interesting that another method of LBO predictions can be derived from the two plotted lines of $q = f(LP)$ and $q_{LBO} = f(LP)$ in Fig. 14. For a given combustor, if $q = f(LP)$ is obtained, q_{LBO} can be easily calculated by the simultaneous equations of $q = f(LP)$ and $q_{LBO} = f(LP)$. That will be investigated further in the future.

6.3. Validation of LBO limit prediction of the combustor using FIA

A validation case of LBO limit prediction using FIA (Combustor 13) is operated. The initial m_f is set as 0.001 kg/s. The computing process of m_f is shown in Table 3.

m_f is considered to be convergent when the variation rate of m_f ($|m_{f,n} - m_{f,n-1}|/m_{f,n}$) is smaller than 0.0005. The fuel mass flow rate at LBO is obtained as $m_{f,n} = 0.002066$, and the FAR at LBO is $q_{LBO,n} = 0.003507$. The prediction uncertainty is about 3.18% ($q_{LBO} = 0.003622$).

Fig. 15 shows the convergent processes of different parameters using FIA. It is shown that the convergent speed of FIA is very fast. An acceptable convergent value of $q_{LBO,n}$ can be obtained within 18 steps.

It is needed to explain that $q_{LBO,n}$ approaches infinitely close to the LBO FAR (0.00356040) calculated by Eq. (2) instead of q_{LBO} (0.003622, obtained by experiment) when $n \rightarrow \infty$. Since Eq. (2) has the high relativity between $V_f \cdot m_f$ and q_{LBO} ($r = 0.97$) and the maximum error in 19 combustors is only $\pm 17.5\%$, the maximum prediction uncertainty of FIA is considered to be also $\pm 17.5\%$. As a comparison to FIA, the Lefebvre's model is used for LBO limit predictions too. The LBO FARs of all the combustors discussed in this

Table 3 Computing process of m_f using FIA for LBO prediction.

n	$m_{f,n}$ (kg/s)	$V_{f,n}$ (10^{-6} m^3)	$m_{r,n}$ (kg/s)	$V_{f,n} \cdot m_{r,n}$ (10^{-7})	$q_{LBO,n} = f$ ($V_{f,n-1} \cdot m_f$)	$ m_{f,n} - m_{f,n-1} /m_{f,n}$
0	0.001000	2.1283	0.002143	0.046	0.002126	
1	0.001252	2.8408	0.003728	0.106	0.002399	0.252296
2	0.001413	3.2183	0.004779	0.154	0.002615	0.128198
3	0.001540	3.4900	0.005623	0.196	0.002807	0.090260
4	0.001653	3.7310	0.006230	0.232	0.002971	0.073341
5	0.001750	3.9239	0.006667	0.262	0.003102	0.058277
6	0.001827	4.0925	0.006972	0.285	0.003210	0.044390
7	0.001890	4.2076	0.007186	0.302	0.003287	0.034540
8	0.001936	4.2965	0.007335	0.315	0.003344	0.023956
9	0.001970	4.3596	0.007441	0.324	0.003386	0.017609
10	0.001994	4.4154	0.007512	0.332	0.003419	0.012480
11	0.002014	4.4626	0.007573	0.338	0.003447	0.009732
12	0.002031	4.5022	0.007623	0.343	0.003471	0.008277
13	0.002045	4.5220	0.007661	0.346	0.003486	0.006929
14	0.002053	4.5401	0.007681	0.349	0.003496	0.004159
15	0.002059	4.5498	0.007697	0.350	0.003503	0.003013
16	0.002063	4.5536	0.007707	0.351	0.003506	0.001889
17	0.002065	4.5556	0.007707	0.351	0.003507	0.000974
18	0.002066					0.000190

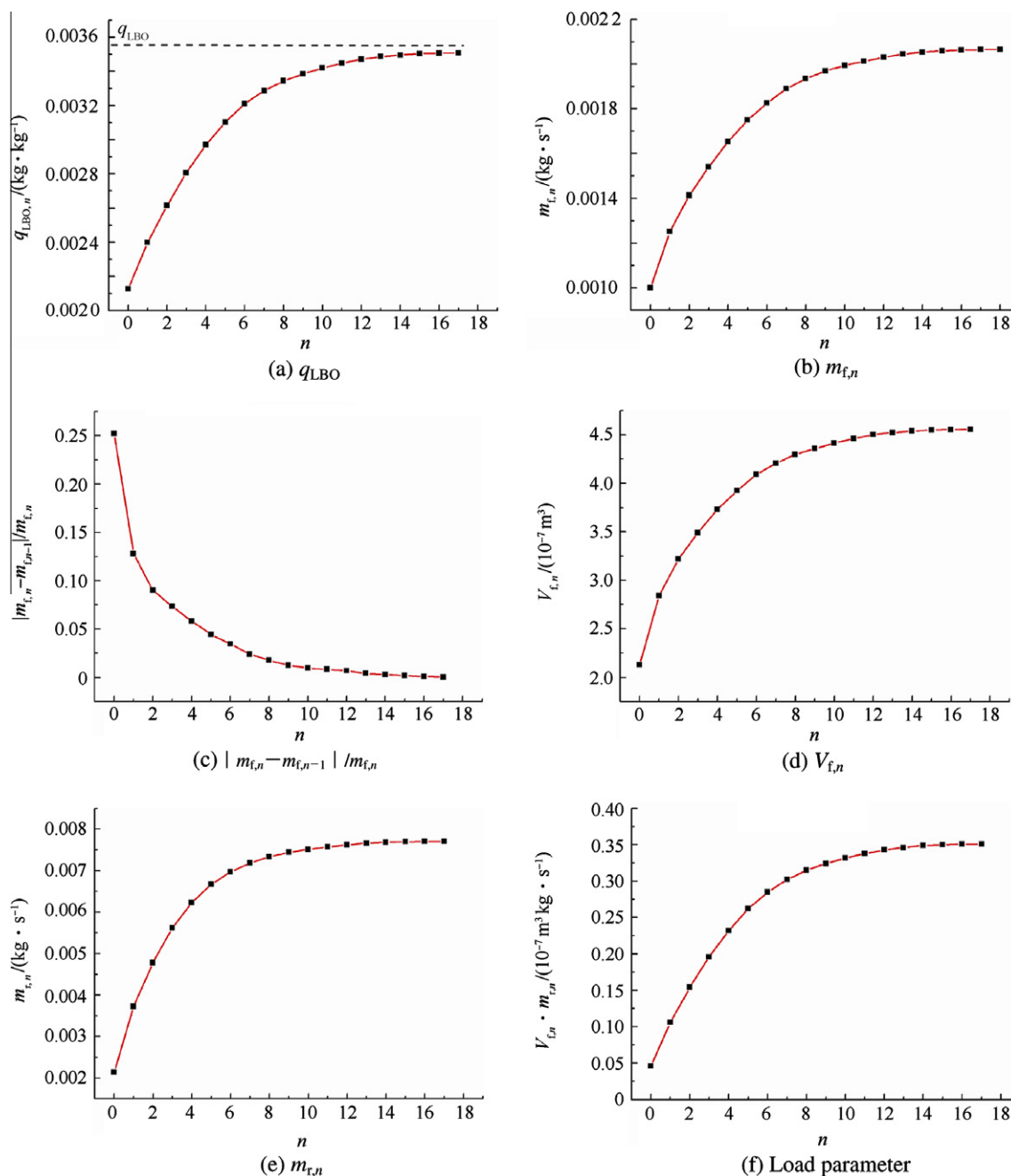


Fig. 15 Convergent processes of different parameters using FIA for LBO prediction.

paper are constant as 0.006 and the prediction uncertainty is $\pm 50\%$.

The time cost of the LBO prediction is relatively low because only the numerical simulation without combustion is operated. The computer equipment used in this study is CPU 2.66 GHz $\times 4$ and 4 GB memory. The convergent time for each m_f adjustment is about 20 min. So the total time cost of LBO prediction for one combustor is about 6 h. If computational grids are reasonably controlled and more computing nodes are used, the time cost will be reduced further.

The work presented here provides combustor designers with a new tool that can help bridge the gap between outdated correlations based on global inputs and complex reacting flow CFD cal-

culations and/or expensive component experimentation. In this paper, the effects of combustor configurations on q_{LBO} are the main concerns, so the properties of fuels as well as the factors of atomization and evaporation are not considered in the load parameter for LBO predictions. In the future, a series of studies about improvement of the load parameter will be operated, so that the load parameter becomes universal.

7. Conclusions

In the present study, a new methodology named FIA is proposed for LBO limit predictions of combustors. Some conclusions are obtained as follows:

- (1) A load parameter of $V_f \cdot m_f$ for LBO analysis is proposed. V_f and m_f are both estimated from the flow field of the combustor that is obtained by numerical simulations without combustion. Comparing with the experiment data, the load parameter ($V_f \cdot m_f$) can represent the actual combustion load of the combustor near LBO and has good relativity with q_{LBO} .
- (2) According to the load parameter, a method named FIA is proposed to make the prediction of q_{LBO} . Comparing with the LBO data for 19 combustors, the results reveals that the LBO FAR obtained by FIA shows good agreement with q_{LBO} , the maximum prediction uncertainty of FIA is about $\pm 17.5\%$.
- (3) The time cost of LBO prediction using FIA for one combustor is about 6 h with the computer equipment of CPU (2.66 GHz) $\times 4$ and 4 GB memory, it is shown that FIA is efficient to be used for practical applications.

References

1. Lefebvre AH. *Gas turbine combustion*. New York: McGraw-Hill Book Company; 1983.
2. Longwell JP, Weiss MA. High temperature reaction rates in hydrocarbon combustion. *Ind Eng Chem* 1955;**47**(8):1634–43.
3. Longwell JP, Frost EE, Weiss MA. Flame stability in bluff body recirculation zones. *Ind Eng Chem* 1953;**45**(8):1629–33.
4. Zukowski EE, Marbel FE. The role of wake transition in the process of flame stabilization on bluff bodies. *AGARD Combust Res Rev* 1955;167–80.
5. Ballal DR, Lefebvre AH. Weak extinction limits of turbulent flowing mixtures. *ASME J Eng Power* 1979;**101**(3):346–51.
6. Ballal DR, Lefebvre AH. Weak extinction limits of turbulent heterogeneous fuel/air mixtures. *J Eng Power* 1980;**102**(2):416–21.
7. Lefebvre AH. Fuel effects on gas turbine combustion-ignition, stability and combustion efficiency. *J Eng Gas Turbines Power* 1985;**107**(1):24–37.
8. Mellor AM. *Design of modern turbine combustors*. London: Academic Press; 1990.
9. Jarymowycz TA, Mellor AM. Correlation of lean blow off in an annular combustor. *J Propul* 1986;**2**(2):190–2.
10. Derr WS, Mellor AM. Characteristic time for lean blow off in turbine combustor. *AIAA Journal* 1979;**17**:1225–33.
11. Leonard PA, Mellor AM. Correlation of lean blow off of gas turbine combustors using alternative fuels. *J Energy* 1983;**7**(6):729–32.
12. Rizk NK, Mongia HC. Gas turbine design methodology. *22nd AIAA/ASME/SAE/ASEE joint propulsion conference 1986-1531*; 1986.
13. Strurgess GJ, Shouse DT. A hybrid model for calculating lean blow-outs in practical combustion. *32nd AIAA/ASME/SAE/ASEE joint propulsion conference 1996-3125*; 1996.
14. Sturgess GJ, Sloan DG, Lesmerises AL. Design and development of a research combustor for lean blow-out studies. *J Eng Gas Turbine Power* 1992;**114**(1):13–9.
15. Sturgess GJ, Gogineni S, Shouse DT. Influence of airblast-atomizing fuel injector design on primary zone flame characteristics at blowout. *AIAA 35th aerospace science meeting and exhibit 1997-0269*; 1997.
16. Black DL, Simth CE. Transient lean blowout modeling of an aerolow emission fuel injector. *39th AIAA/ASME/SAE/ASEE joint propulsion conference 2003-4520*; 2003.
17. Menon S, Eggenspieler G, Patel N. Structure of locally quenched swirl stabilized turbulent premixed flame. *42nd AIAA aerospace sciences meeting and exhibit 2004-0979*; 2004.
18. Menon S, Stone C, Patel N. Multi-scale modeling for LES of engineering designs of large-scale combustors. *42nd AIAA aerospace sciences meeting and exhibit 2004-0157*; 2004.
19. Kim WW, Lienau JL, Slooten PRV. Towards modeling lean blowout in gas turbine flame holder application. *J Eng Gas Turbine Power* 2006;**128**(1):40–8.
20. Knaus DA, Patrick JM, Roger WH, Phillips SC, Kiel BV. Improved correlations for augmentor static stability. *45th AIAA aerospace sciences meeting and exhibit 2007-0389*; 2007.
21. Knaus DA, Patrick JM, Roger WH, Phillips SC, Kiel BV. Predicting augmentor static stability using local Damköhler number. *47th AIAA aerospace sciences meeting and exhibit 2008-1027*; 2008.
22. Smith CE, Dan Nickolaus, Timothy Leach, Kiel BV, Garwick K. LES blowout analysis of premixed flow past V-gutter flameholder. *45th AIAA aerospace sciences meeting and exhibit 2007-170*; 2007.
23. Wang HR, Jin J. Lean blowout predictions of a non-premixed V-Gutter stabilized flame using a Damköhler number methodology. *Proc ASME Turbo Expo* 2011.
24. Roach JM, Fisher TC, Frankel SH. CFD predictions of Damköhler number fields for reduced order modeling of V-Gutter flame stability. *46th AIAA aerospace sciences meeting and exhibit 2008-509*; 2008.
25. Shanbhogue SJ, Husain S, Lieuwen T. Lean blowoff of bluff body stabilized flames: scaling and dynamics. *Prog Energy Combust Sci* 2009;**35**(1):98–120.
26. Poinso T, Veynante D. *Theoretical and numerical combustion*. Philadelphia, PA, USA: R.T. Edwards Inc.; 2005.
27. Xie F, Huang Y, Wang F, Hu B. Visualization of the lean blowout process in a combustor with swirl cup. *Proc ASME turbo expo* 2010.
28. *Fluent 6.3 User's Guide*. Fluent Inc.; 2006.
29. Davoudzadeh F, Liu NS, Moder JP. Investigation of swirling air flows generated by axial swirlers in a flame tube. *Proc ASME turbo expo* 2006.
30. Dezubay EA. Characteristic of disk-controlled flame. *Aero Digest* 1950;**61**(1):54–6.
31. King CR. A semi-empirical correlation of afterburner combustion efficiency and lean-blowout fuel-air-ratio data with several afterburner-inlet variables and afterburner lengths. *NACA RME57F26* 1957.
32. *Handbook of Jet Fuel Performance*. Beijing: Research Institute of Petroleum Processing; 1984 [Chinese].

Hu Bin received his Ph.D. degree from Beihang University in 2012, and then became an assistant professor in the Institute of Engineering Thermophysics at the Chinese Academy of Sciences. His main research interests are combustion and combustors.

Wang Fang received her Ph.D. degree from Tsinghua University in 2007, and then became an assistant professor in the School of Energy and Power Engineering, Beihang University. Her main research interests are numerical simulation and turbulent flow.